(NASA-TM-82131) EVALUATION OF MAGNETIC HELICITY IN HOMOGENEOUS TURBULENCE (NASA) 15 p HC A02/MF A01 CSCL 20I

N81-23900

Unclas
G3/75 24301

NASA

Technical Memorandum 82131

Evaluation of Magnetic Helicity in Homogeneous Turbulence

W. H. Matthaeus, M. L. Goldstein, and C. Smith

APRIL 1981

National Aeronautics and Space Administration

Goddard Space Flight Center
Greenbelt, Maryland 20771

EVALUATION OF MAGNETIC HELICITY IN HOMOGENEOUS TURBULENCE

by

William H. Matthaeus[(a)]

and

Melvyn L. Goldstein

NASA/Goddard Space Flight Center
Code 692, Laboratory for Extraterrestrial Physics
Greenbelt, MD 20771

and

Charles Smith

Department of Physics
The College of William and Mary
Williamsburg, VA 23185

Submitted to Physical Review Letters.
PACS numbers: 52.30.+r, 52.35.Ra, 94.60.Da

ABSTRACT

We present a technique for the measurement of magnetic helicity from values of the two point magnetic field correlation matrix under the assumption of spatial homogeneity. Knowledge of a single scalar function of space, derivable from the correlation matrix, suffices to determine the magnetic helicity. We illustrate the technique by reporting the first measurement of the magnetic helicity of the solar wind.

A considerable body of theoretical plasma physics literature over the last twenty-five years has emphasized the importance of magnetic helicity, defined as

$$H_m \equiv \int \underset{\sim}{A} \cdot \underset{\sim}{B} d^3x \qquad (1)$$

where $\underset{\sim}{B}$ and $\underset{\sim}{A}$ are the magnetic field and the vector potential, respectively. This integral extends over all field containing regions, and $\underset{\sim}{A}$ is subject to the gauge condition $\nabla \cdot \underset{\sim}{A} = 0$. H_m may also be defined "per unit volume" so that $H_m \equiv \langle \underset{\sim}{A} \cdot \underset{\sim}{B} \rangle$. The magnetic helicity measures the departure of a turbulent magnetic field from mirror symmetry, or equivalently, the degree of topological linkage of magnetic flux tubes[1].

Woltjer[2] noticed that under fairly general assumptions H_m is an integral invariant of the incompressible one fluid ideal magnetohydrodynamic (MHD) equations. He then developed a variational formulation for calculating MHD equilibria[3] which Taylor[4] and Montgomery *et al.*[5] applied to MHD dynamics in a conducting cylinder. Their "relaxation theory" has been used in the MHD theory of Reversed Field Pinch plasma confinement devices[6].

Turbulence theory has also addressed the dynamical role of magnetic helicity. Frisch *et al.*[7], in analogy to two-dimensional turbulence theory[8,9], conjectured that an inverse cascade of magnetic helicity may be characteristic of three-dimensional MHD flows. In steady state, with helicity and energy supplied at a constant rate to intermediate wavenumbers, an MHD system would then consist of two inertial ranges: an inverse cascade of magnetic helicity to large scales, and a direct cascade of energy to small scales. A class of selective decay hypotheses has been discussed[8,10] which states that the large

Reynolds number, non steady dynamics, of a two rugged invariant system are characterized by the rapid decay of the direct transfer quantity and preservation of the back transfer quantity.

The conjectured implications for three-dimensional MHD are that: 1), the ratio of energy to magnetic helicity decreases in time; 2), in the limit of extremely high Reynolds numbers the ratio approaches a limit defined by the geometry; and 3), the net magnetic helicity resides primarily in the largest scales of the system, regardless of its scale in the initial conditions.

Our understanding of the dynamical importance of H_m and the range of validity of the relaxation, inverse cascade and selective decay theories is limited by the lack of interplay between theory and experiment. We are not aware of a single direct measurement of magnetic helicity or its spectrum. Thus, it is desirable to develop procedures for obtaining magnetic helicity from experiments. In this letter we present a straightforward procedure for evaluating magnetic helicity from values of the two point magnetic field correlation matrix $R_{ij}(\underset{\sim}{r})$ under the assumption that the statistical properties are spatially homogeneous.

We begin with the definition

$$R_{ij}(\underset{\sim}{r}) = \langle B_i(\underset{\sim}{x}) B_j(\underset{\sim}{x}+\underset{\sim}{r}) \rangle \tag{2}$$

where the brackets denote an appropriate average over a statistical ensemble. The assumption of "weak" homogeneity renders R_{ij} a function only of the spatial separation $\underset{\sim}{r}$; thus $R_{ij}(\underset{\sim}{r}) = R_{ji}(-\underset{\sim}{r})$. R_{ij} also satisfies the solenoidal condition

$$\frac{\partial}{\partial r_j} R_{ij}(\underset{\sim}{r}) = \frac{\partial}{\partial r_i} R_{ij}(\underset{\sim}{r}) = 0 \tag{3}$$

where summation is implied by repeated indices. As discussed in Ref. 11, $R_{ij}(\underset{\sim}{r})$ may always be additively decomposed into a symmetric proper tensor $T_{ij}(\underset{\sim}{r})$ with even spatial parity and an antisymmetric pseudotensor $P_{ij}(\underset{\sim}{r})$ with odd spatial parity.

The transformation properties of a homogeneous, solenoidal correlation matrix R_{ij} uniquely determine the form of the pseudotensor $P_{ij}(\underset{\sim}{r})$ as can be seen by use of the method of isotropic tensors introduced by Robertson and others[12]. By using all available vectors and the isotropic forms δ_{ij} and ϵ_{ijk}, one may exhaustively list the linearly independent tensor forms available for inclusion in R_{ij}. The required manipulations are easier to perform in Fourier space employing the energy spectrum tensor

$$S_{ij}(\underset{\sim}{k}) = (\frac{1}{2\pi})^3 \int d\underset{\sim}{r}\, e^{-i\underset{\sim}{k}\cdot\underset{\sim}{r}}\, R_{ij}(\underset{\sim}{r}) \qquad (4)$$

If no rotational or reflectional symmetries are assumed, the solenoidal constraint leads to 31 k-space tensor forms at the onset[13]. These depend on $\underset{\sim}{k}$ and two independent principal axis unit vectors. The Fourier space pseudotensor, odd under $\underset{\sim}{k} \to -\underset{\sim}{k}$, must be antisymmetric in its indices; similarly, the proper tensor is even and symmetric. Simple algebraic manipulations show that only three pseudctensors can be linearly independent. The solenoidal constraint eliminates two of these leaving one form, $\epsilon_{ijm}k_m G(\underset{\sim}{k})$, where G is a scalar function of $\underset{\sim}{k}$, satisfying $G(\underset{\sim}{k}) = G(-\underset{\sim}{k})$. Additional symmetries imposed on the system can only modify the way in which G depends on $\underset{\sim}{k}$, but cannot introduce additional functions into the form of the k-space pseudotensor. Likewise in configuration space, P_{ij} is derivable from a single scalar function $\phi(\underset{\sim}{r})$, and has the form

$$P_{ij}(\underset{\sim}{r}) = \epsilon_{ijm} \frac{\partial}{\partial r_m} \phi(\underset{\sim}{r}) \tag{5}$$

The fact that P_{ij} depends only on the gradient of a single scalar function of $\underset{\sim}{r}$ provides the basis for determining the magnetic helicity.

Let the ij^{th} component of the Fourier transform of the symmetric part of the $\langle \underset{\sim}{B}\, \underset{\sim}{A} \rangle$ correlation be denoted H_{ij}. Then, using Eq. (4), $H_{ij}(\underset{\sim}{k})$ is[14]

$$H_{ij}(\underset{\sim}{k}) = i\epsilon_{jrs} k_r S_{is}(\underset{\sim}{k})/k^2 \tag{6}$$

Because H_m is the trace of $\langle \underset{\sim}{B}\, \underset{\sim}{A} \rangle$ evaluated at $\underset{\sim}{r} = 0$ (Eq. 1), we immediately have

$$H_m = \int d\underset{\sim}{k}\, H_{jj}(\underset{\sim}{k}). \tag{7}$$

From Eq. (6) and (7), we now see that $H_{jj}(\underset{\sim}{k})$ is the spectrum of magnetic helicity, $H_m(\underset{\sim}{k})$. Furthermore, because $H_m(\underset{\sim}{k})$ depends solely on the antisymmetric part of S_{ij}, $G(\underset{\sim}{k}) = iH_m(\underset{\sim}{k})/2$. Finally, from Eq. (1) and (5), we have the desired expression for H_m, *viz.*,

$$H_m = \langle \underset{\sim}{A} \cdot \underset{\sim}{B} \rangle = 2\phi(\underset{\sim}{r} = 0) \tag{8}$$

The function $\phi(\underset{\sim}{r})$, which determines both the total magnetic helicity and its spectrum, may be evaluated by performing a line integral over separation values:

$$2\phi(\underset{\sim}{r}) = 2 \int_{\underset{\sim}{0}}^{\underset{\sim}{r}} \nabla\phi \cdot d\underset{\sim}{\ell} = \int_{\underset{\sim}{0}}^{\underset{\sim}{r}} d\ell_i\, \epsilon_{ijm} R_{jm}(\underset{\sim}{\ell}) \tag{9}$$

Eq. (9) is valid provided that the correlations vanish rapidly as $|\underset{\sim}{r}| \to \infty$. H_m is then given by Eq. (8).

To determine $H_m(\underset{\sim}{k})$, one must Fourier transform Eq. (9), which requires exhaustive knowledge of ϕ for all $\underset{\sim}{r}$. However, a <u>reduced</u> helicity spectrum is available from knowledge of $R_{ij}(r_1,0,0)$, the correlation tensor for a sequence of collinear separations in the r_1 direction. The reduced energy spectrum tensor[13] is defined as

$$S^r_{ij}(k_1) = \frac{1}{2\pi} \int dr_1 \, e^{-ik_1 r_1} \, R_{ij}(r_1,0,0) \qquad (10)$$

$$= \int dk_2 dk_3 \, S_{ij}(k_1,k_2,k_3)$$

so that

$$H^r_m(k_1) = \frac{1}{2\pi} \int dr_1 \, \phi(r_1,0,0) \, e^{-ik_1 r_1} \qquad (11)$$

$$= 2 \, \mathrm{Im} \, S^r_{23}(k_1)/k_1$$

and

$$H_m = \int dk_1 \, H^r_m(k_1) = 2\phi(r_1=0,0,0) \qquad (12)$$

Application of these results to fusion plasmas may be limited by strong inhomogeneities present in a bounded laboratory device. However, in the laboratory one can interpret the ensemble average as an average over identically prepared "shots" of a containment device, which may permit useful values of helicity to be extracted. Magnetic helicity can also be measured in space plasmas. We have used magnetometer data from the Voyager 2 spacecraft in the solar wind near 2.8 astronomical units (AU). The results reported here are

from a single span of 64 hours on days 95 - 97 of 1978. This is a single point measurement in a highly super-Alfvénic flow, which justifies use of the MHD analogue of the frozen flow approximation to obtain $S^r_{ij}(k)$.

We evaluated $S^r_{ij}(k)$ via two independent means: the Blackman-Tukey (BT) mean lagged product technique with 24 degrees of freedom, and the Fast Fourier Transform (FFT) technique smoothed to have equivalent statistical validity. The two techniques gave essentially identical results. Tests were made to eliminate the possibility that aliasing or leakage affected the analysis. The results shown in Fig. 1 and 2 were obtained with the FFT approach.

Fig. 1 displays both the reduced magnetic energy density $E(k) = S^r_{ii}(k)$ and $|kH_m(k)|$ (cf. Eq. 12) in units of γ^2 ($1\ \gamma = 10^{-5}$ Gauss). (In converting from frequency to wavenumber, we used the solar wind speed during this period which was 450 km/s. In the following discussion, the superscript on the reduced helicity is omitted.

As has often been reported, E(k) closely approximates a power law (the slope in this case is -1.7 ± 0.1). The notable feature in Fig. 1 is that the envelope of $|kH_m(k)|$ closely traces the same power law. Note that there is no tendency for $|kH_m(k)|/E(k)$ to become small at large k. In fact, $kH_m(k)$ oscillates between $\approx \pm 0.4$ of its maximal values throughout the spectrum. Nevertheless, the net helicity density ($\approx 18\ G^2$ cm) is entirely due to the helicity in the largest scale fluctuations. The helicity containing length ($2\pi H_m/\Sigma kH_m(k)$) is about 9.9×10^{12} cm compared with the similarly defined energy containing length ($2\pi E/\Sigma kE(k)$), which is $\approx 5 \times 10^{11}$ cm. The correlation length[18] ($\int R_{ii}dr/E$) for this data set is 2.5×10^{12} cm.

The high degree of correlation and anticorrelation between E(k) and $H_m(k)$ is illustrated in Fig. 2 where $k^{5/3}E(k)$ and $k^{8/3}H_m(k)$ are plotted against both frequency and wavenumber. Because of the linear scale, Fig. 2 emphasizes the

high frequency behavior of $H_m(k)$. These results suggest that the solar wind during this period is rich in helical structures; exhibiting a significant twist to the magnetic field at very large scales. Large clumps of positive and negative helicity are also found at all smaller scales, but with an average value close to zero. A detailed analysis of the solar wind magnetic field structure at several locations in the heliosphere will be presented in a more complete paper.

We thank the Voyager magnetometer team for help and cooperation in the data analysis, W. H. Mish for aid with the numerical analysis, and D. Montgomery for many stimulating conversations. The participation of C. Smith was supported in part by National Aeronautics and Space Administration grant NSG-7416.

(a) NAS/NRC Resident Postdoctoral Research Associate

[1] H. K. Moffatt, Magnetic Field Generation in Electrically Conducting Fluids, (Cambridge Univ. Press, 1978), Sec. 2.1.

[2] L. Woltjer, Proc. Nat. Acad. Sc. 44, 489 (1958).

[3] L. Woltjer, Proc. Nat. Acad. Sc. 45, 769 (1959).

[4] J. B. Taylor, in Plasma Physics and Controlled Fusion, I, 161, IAEA, Vienna 1975

[5] D. Montgomery, L. Turner and G. Vahala, Phys. Fluids 21, 757 (1978).

[6] Proceedings of the Reversed Field Pinch Theory Workshop, Los Alamos Scientific Laboratory, April 28-May 2, 1980.

[7] U. Frisch, A. Pouquet, J. Leorat and A. Mazure, J. Fluid Mech. 68, 769 (1975).

[8] G. K. Batchelor, Phys. Fluids Suppl. II, 233 (1969).

[9] R. H. Kraichnan, Phys. Fluids 10, 1417 (1967), and J. Fluid Mech. 67, 155 (1975).

[10] W. Matthaeus and D. Montgomery, in Ann. N. Y. Acad. Sci. 357, 203 (1981).

[11] W. Matthaeus and C. Smith, NASA Technical Memorandum 82048 (1980), submitted to Phys. Rev. A.

[12] H. P. Robertson, Proc. Camb. Phil. Soc. 36, 209 (1940).

[13] G. K. Batchelor, Theory of Homogeneous Turbulence, (Cambridge Univ. Press, 1970).

[14] D. Montgomery and L. Turner, Phys. Fluids, in press (1981).

FIGURE CAPTIONS

Fig. 1. The reduced magnetic energy density E(k) and the reduced helicity spectrum $|kH_m(k)|$ (in energy units) of the solar wind at 2.8 AU. The solar wind velocity as 450 km/s, and the total fluctuation energy is 4.8×10^{-12} ergs/cm^3. E(k) has a power law slope of $k^{-1.7 \pm 0.1}$. For clarity, not all values of $H_m(k)$ are plotted at high frequencies.

Fig. 2. E(k) and $H_m(k)$ plotted on a linear scale for the data shown in Fig. 1. The top trace is $k^{5/3}E(k)$; the bottom trace is $k^{8/3}H_m(k)$.

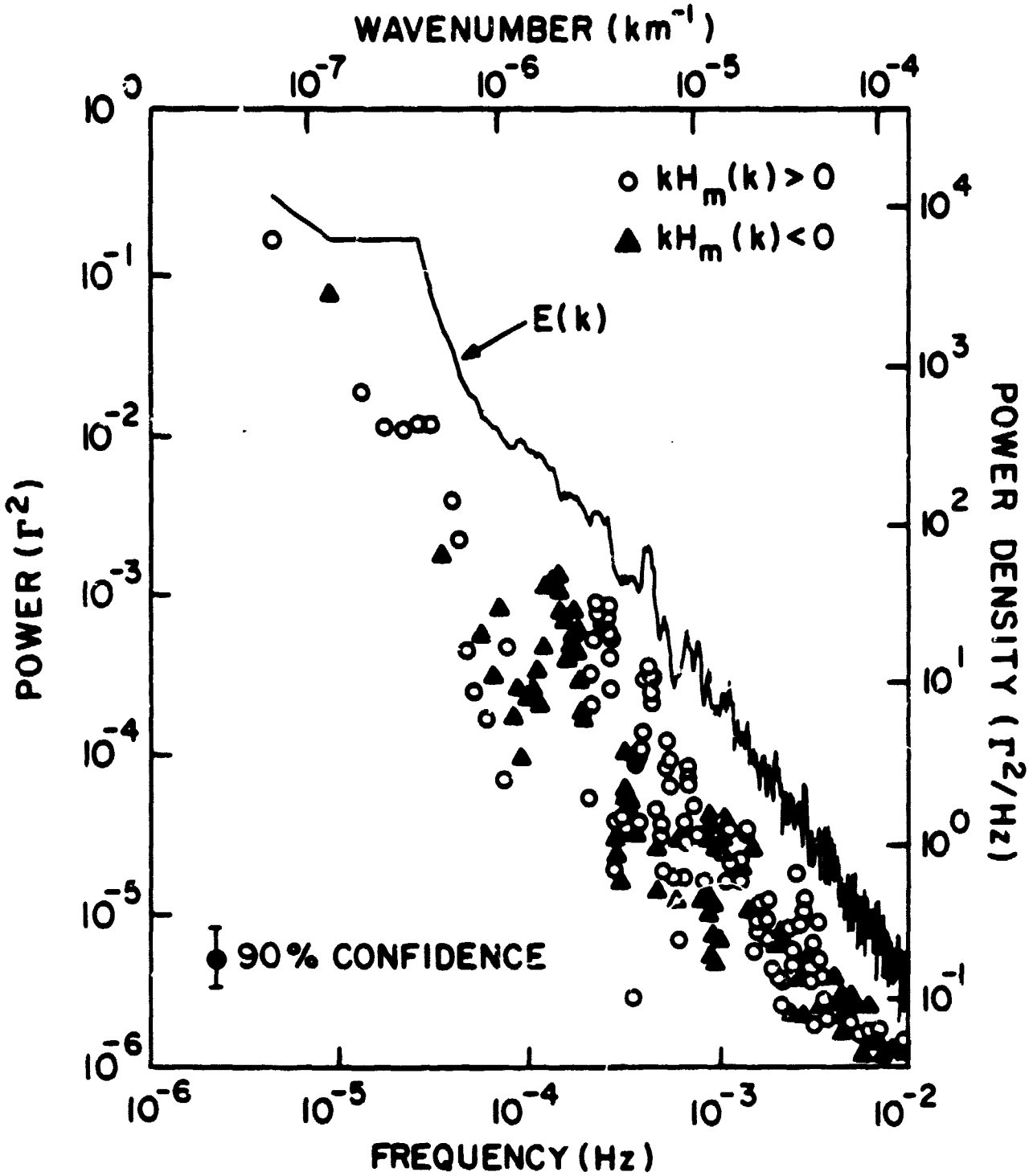
WAVENUMBER (km⁻¹)
10⁻⁷
10⁻⁶
10⁻⁵
10⁻⁴
10⁰
10⁻¹
10⁻²
10⁻³
10⁻⁴
10⁻⁵
10⁻⁶
o kH_m(k)>0
▲ kH_m(k)<0
E(k)
90% CONFIDENCE
POWER (r²)
POWER DENSITY (r²/Hz)
10⁴
10³
10²
10¹
10⁰
10⁻¹
10⁻⁶
10⁻⁵
10⁻⁴
10⁻³
10⁻²
FREQUENCY (Hz)

Figure 1

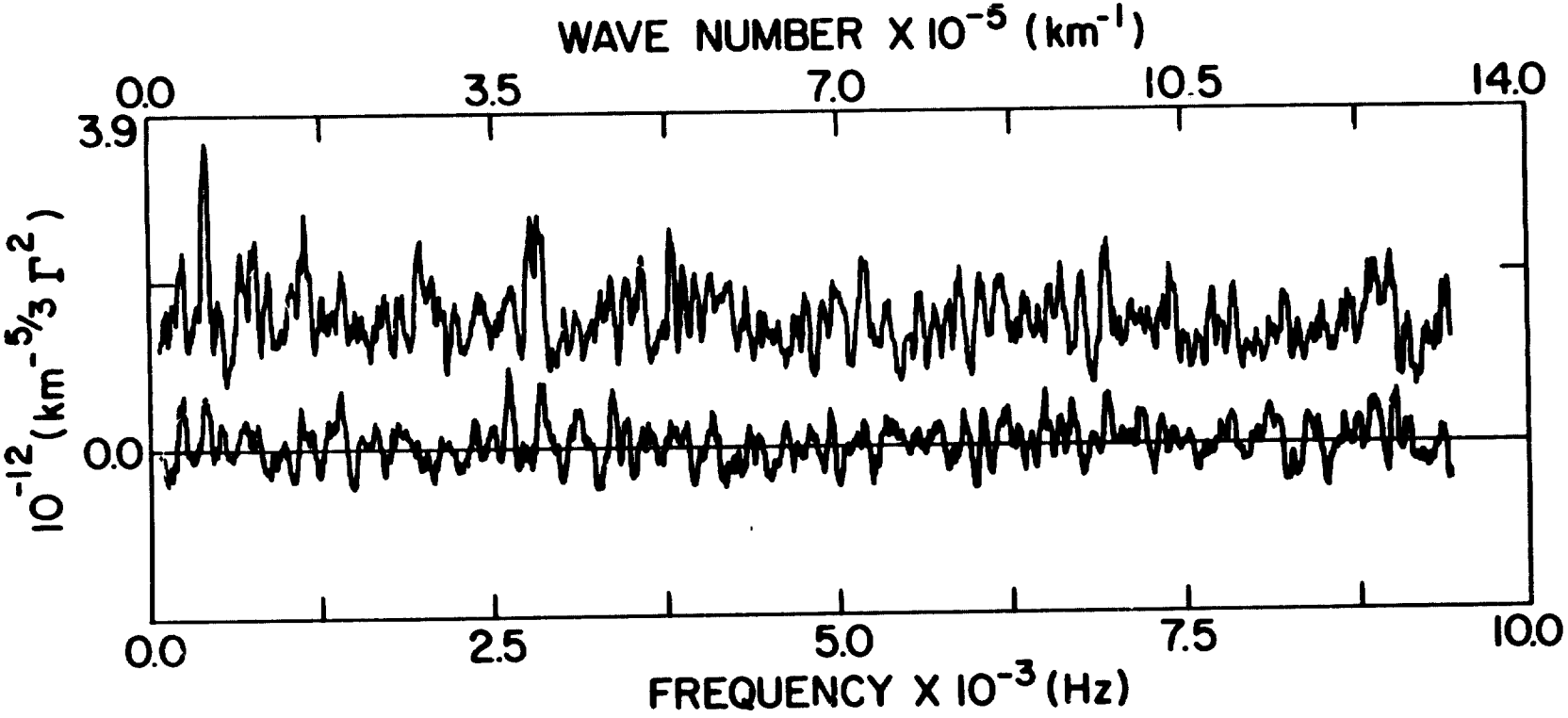
WAVE NUMBER X 10^-5 (km^-1)
0.0
3.5
7.0
10.5
14.0
3.9
0.0
10^-12 (km^-5/3 Γ^2)
0.0
2.5
5.0
7.5
10.0
FREQUENCY X 10^-3 (Hz)

Figure 2